JOURNAL OF MATERIALS SCIENCE 27 (1992) 5953–5957

Optical and electronic properties of cobalt-doped zinc oxide films prepared by the sputtering method

K. KOBAYASHI, T. MAEDA, S. MATSUSHIMA, G. OKADA
Department of Applied Chemistry, Faculty of Engineering, Ehime University, Matsuyama 790, Japan

In-doped ZnO, Co-doped ZnO and Li-doped NiO are successively deposited on quartz by the sputtering method. A current versus voltage curve of the three-layer device, in which the In-doped ZnO and Li-doped NiO are used as electrodes, reveals that the In-doped ZnO is an ohmic electrode and the Li-doped NiO is a blocking electrode with respect to electron injection. In photocurrent spectra of the three-layer device, there are two distinct peaks around 410 and 640 nm. The former is ascribed to the photoionization caused by the electric-dipole transition from the ground states, $^4A_2(F)$, to the conduction band, and the latter to the thermal emission from electronic excited states of Co^{2+}, $^4T_1(P)$.

1. Introduction

Photochromism has attracted considerable attention as an optical memory [1, 2]. In inorganic photochromic materials, transition metal ions are introduced into an oxide with a fairly large band gap. In such inorganic photochromic materials, impurity levels arising from doped transition metal ions are formed in the band gap of a host material [3]. The change in optical absorption due to doped impurities is caused by the charge transfer between impurity levels and the conduction (valence) band. Thus, the investigation of the charge transfer between impurity levels and the conduction (valence) band in an inorganic photochromic material is required to clarify the mechanism of photochromism in inorganic materials.

In the present work, we are interested in Co-doped ZnO as a photochromic material because ZnO, the host material, has a wide band gap and no inversion symmetry, which is one of the important preconditions for optical absorption of the electric dipole transition. A device was fabricated having a three-layer structure of an electrode, the Co-doped ZnO and an electrode. Using this three-layer device, spectral dependence of photocurrent of the Co-doped ZnO is measured by applying a strong electric field between the two electrodes in the device. On the basis of the photocurrent spectra, the charge transfer between Co impurity levels and the conduction (valence) band of ZnO is discussed.

2. Experimental procedure

A Co-doped ZnO powder as a target in the sputtering was prepared by sintering the mixture of ZnO (99.99%), 5 mol% LiO (99.5%) and 5 mol% CoO (99.9%) at 900 °C for 3 h in air (Li atoms were introduced to increase the resistivity of ZnO). An In-doped ZnO powder was prepared by sintering the mixture of ZnO and 5 mol% In_2O_3 (99.9 %) at 900 °C for 3 h in air. A Li-doped NiO powder was prepared by sintering NiO (99.9%) and 5 mol% LiO at 900 °C for 3 h in air. The sputtering was carried out using a planar magnetron sputtering apparatus (Tokki SPK-201). The thickness of a film deposited on quartz was estimated from the interference in absorption spectra in the range 200–900 nm. A device with three-layer structure was fabricated by successive sputtering of In-doped ZnO, Co-doped ZnO and Li-doped NiO on quartz substrate. Ag wires were connected to both the In-doped ZnO and the Li-doped NiO with Ag paste. Diffuse reflection spectra of the Co-doped ZnO powder were measured using a photospectrometer (Beckman UV5240). Photocurrent spectra were measured with a light chopper, a lock-in amplifier and a monochromatic irradiation apparatus (Jasco CRM-FA) including a 2 kW Xe lamp as a light source.

3. Results

To examine the optical properties and crystal structure of sputtered films, such films were prepared of In-doped ZnO, Co-doped ZnO and Li-doped NiO on quartz substrates. The sputtering conditions are listed in Table I. Fig. 1 shows the X-ray diffraction (XRD) patterns of the In-doped ZnO and Co-doped ZnO films. For the In-doped ZnO film, only the intense (0 0 2) and weak (0 0 4) reflections of ZnO are observed in the XRD. For the Co-doped ZnO film, there exist (1 0 0) and (1 0 1) reflections besides (0 0 2) and (0 0 4) reflections in the XRD. No reflections related to Co or In compounds are seen in both the XRD of the In-doped ZnO and Co-doped ZnO films. Thus, In or Co ions in these sputtered films are introduced into the

0022–2461

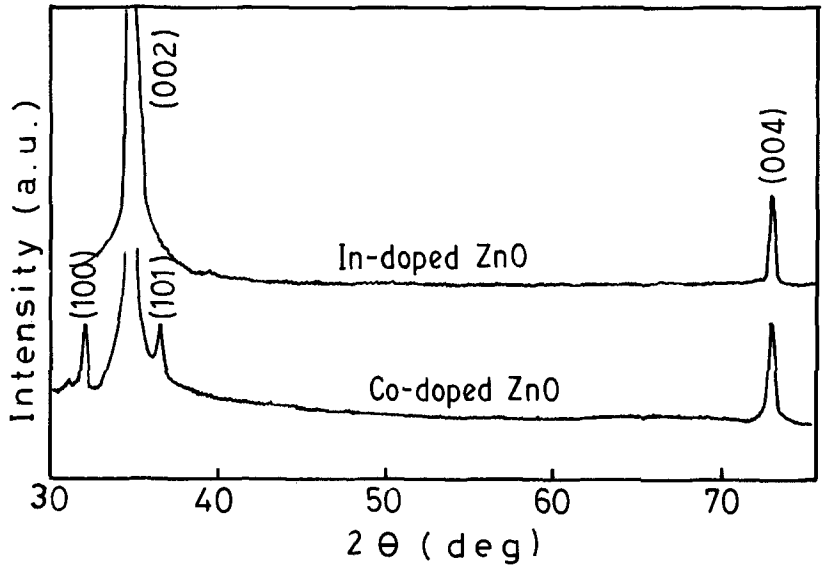

Figure 1 X-ray diffraction patterns of In-doped ZnO and Co-doped ZnO sputtered films.

TABLE I Sputtering conditions of In-doped ZnO, Co-doped ZnO and Li-doped NiO films

	In-doped ZnO	Co-doped ZnO	Li-doped NiO
Pressure (Pa)	0.66	0.66	0.66
RF power (W)	75	75	75
Gas	Ar	Ar	Ar
Substrate temperature (°C)	400	400	–[a]
Film thickness (nm)	1000	1200	---[b]
Sputter time (h)	2	3	0.5
Deposition rate (nm h^{-1})	500	400	---

[a] Substrate was not heated intentionally.
[b] The film thickness cannot be estimated.

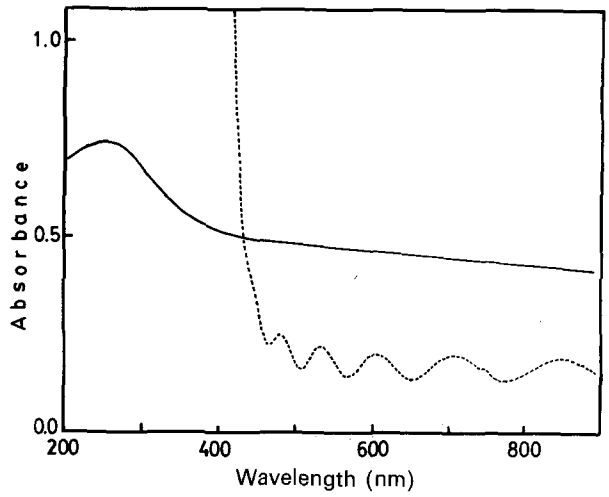

Figure 2 Absorption spectra of In-doped ZnO (---) and Li-doped NiO (——) sputtered films.

ZnO lattice. The *c*-axis of the In-doped ZnO film is preferentially oriented perpendicular to the substrate surface. The appearance of (1 0 0) and (1 0 1) reflections in the XRD for the Co-doped ZnO film may result from doped Co ions. The Co-doped ZnO film is an insulator, while the In-doped ZnO film and the Li-doped NiO film have a surface resistance of 10 and 200 k Ω, respectively.

Fig. 2 shows absorption spectra of the In-doped ZnO and the Li-doped NiO films deposited on a quartz substrate. Many waves due to interference are observed in the absorption spectrum of the In-doped ZnO film. From the interval between two peaks, the film thickness is estimated to be 1000 nm for the In-doped ZnO film. For the Li-doped NiO, no interference effect is seen in the absorption spectra because of stronger absorption. The absorption peak near 300 nm is probably attributed to the band-gap excitation of NiO [4, 5]. Strong absorption in the visible and near infrared regions caused by the doping of Li into NiO may result from free carriers (Drude type) and from the intra p–p transition in the valence band, as well as superconducting cuprate compounds [6].

Fig. 3 shows the absorption spectrum of the Co-doped ZnO film and the reflection spectrum of the Co-doped ZnO powder used for a target in the sputtering. From the interval between peaks, the film thickness is estimated to be 1200 nm for the Co-doped ZnO films. An undoped ZnO film is transparent in the visible region, while the Co-doped ZnO film is greenish. The extra absorption peak around 600 nm of the Co-doped ZnO film is the origin of the colour of the film. Nevertheless, the interference effect makes it difficult to determine an accurate wavelength of the absorption peak. Information on absorption spectra can be obtained from the diffuse reflection spectrum of the Co-doped ZnO powder (the reflectivity is related to the absorbance by the Kubelka–Munk function). As seen in Fig. 3, three dips in the reflection spectrum at 570, 610 and 660 nm correspond to absorption peaks of a single crystal of Co-doped ZnO. The absorption peaks at 660 and 570 nm have been assigned to the transitions from the ground state of $^4A_2(F)$ to $^2E(G)$ and to $^2A_1(G)$ [7–9], where symbols A_2, E and A_1 stand for the irreducible representation in T_d symmetry, and symbols in parentheses stand for spectroscopic notations of free ions. The broad absorption around 600 nm has been attributed to

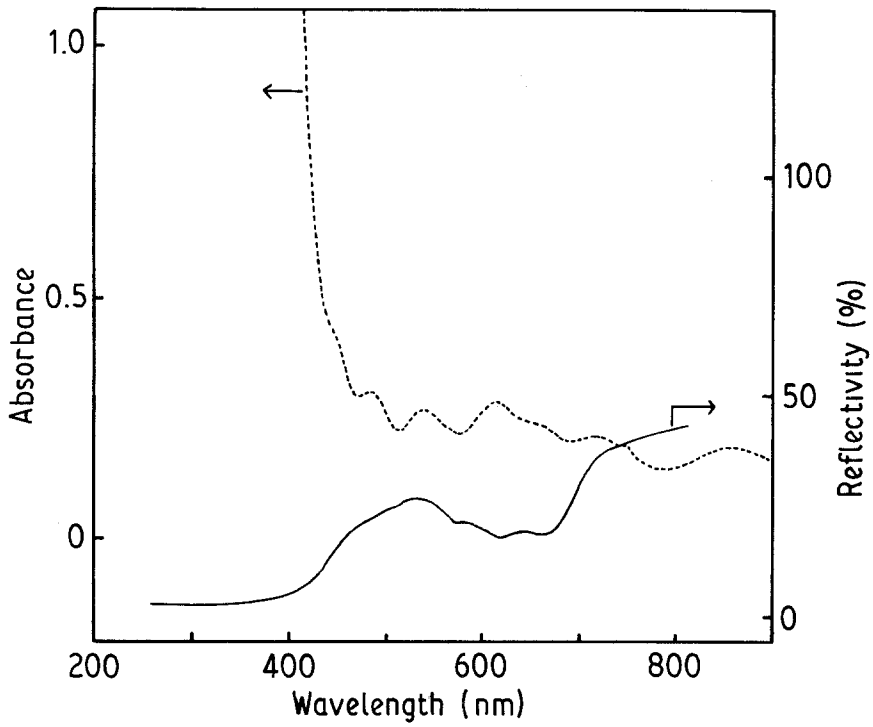

Figure 3 Absorption spectrum (---) of Co-doped ZnO sputtered films and reflection spectrum (——) of Co-doped ZnO powder.

overlap of the transition from $^4A_2(F)$ to $^4T_1(P)$ and the transition from $^4A_2(F)$ to $^2T_1(G)$ [7–9].

To measure the spectral dependence of photocurrent of the Co-doped ZnO film, a three-layer device was fabricated on quartz substrate: In-doped ZnO, Co-doped ZnO and Li-doped NiO films were successively deposited on a quartz substrate by sputtering. The schematic illustration of the three-layer device is shown in Fig. 4. The thickness of the In-doped ZnO and Co-doped ZnO films is 250 and 800 nm, respectively. A curve of current versus voltage of the three-layer device in the dark is shown in Fig. 5. As seen in Fig. 5, the current versus voltage (I–V) curve is unsymmetrical: the I–V curve is linear at a forward bias voltage where a voltage is applied such that the In-doped ZnO electrode is negative with respect to the Li-doped NiO electrode. In contrast, the I–V curve at a reverse bias voltage is non-linear and the magnitude of current tends to saturate at a voltage higher than 10 V. This unsymmetrical I–V curve leads to the conclusion that the In-doped ZnO is an ohmic electrode for the electron injection into the conduction band of the Co-doped ZnO, while the Li-doped NiO is a blocking electrode for the electron injection. In other words, the rate-limited process is the electron injection from the Li-doped NiO in the reverse bias, but is the charge flow in the bulk of the Co-doped ZnO in the forward bias. The characteristics of the two electrodes are consistent with the theoretical prediction deduced from the Fermi level of the two electrodes; the Fermi levels of the In-doped ZnO and the Li-doped NiO are

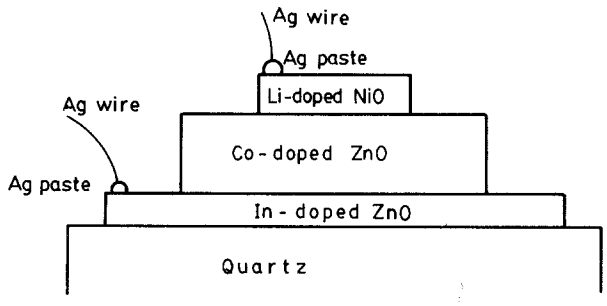

Figure 4 Schematic illustration of a three-layer device.

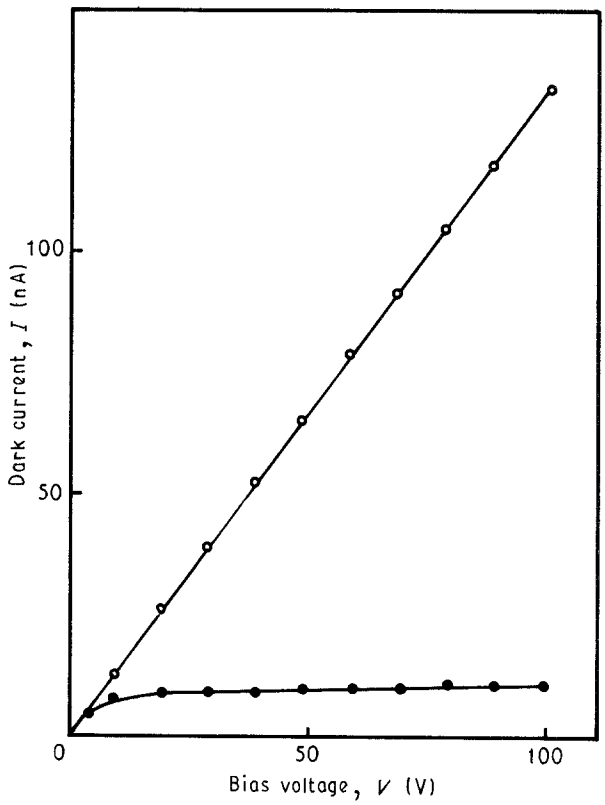

Figure 5 Current versus voltage curve of the three-layer device in the dark. ○, Forward bias; ●, reverse bias.

located near the conduction band of ZnO and near the top of the valence band of NiO [10, 11].

Spectral dependence of photocurrent of the three-layer device at a reverse bias voltage of 100 V is shown in Fig. 6. The photocurrent is normalized by the number of photons of light incident at the device surface. The noticeable feature of the photocurrent spectra of the Co-doped ZnO is that two distinct peaks appear around 410 and 640 nm, and that no photocurrent is observed at a wavelength longer than 720 nm. These peaks at 410 and 640 nm are not observed for a three-layer device consisting of In-doped ZnO, undoped ZnO and Li-doped NiO. Thus, these peaks in the photocurrent spectrum are associated with Co ions doped into ZnO. The observation that no photocurrent flows at a wavelength longer that 720 nm is significantly different from the spectral dependence of the photoconductivity of Co-doped ZnO [12]: the photoconductivity was observed over the range 1000–3000 nm. This difference is attributable to the characteristic of the Li-doped NiO as a blocking electrode. In photocurrent measurements at a reverse bias voltage, the rate-limiting process is the electron injection from the Li-doped NiO electrode into the conduction band of the Co-doped ZnO. Thus, the variation in the bulk conductivity caused by light absorption, i.e. photoconductivity, has no influence on the total current. However, this situation is significantly modified when free holes are generated in the valence band of the Co-doped ZnO because the Li-doped NiO behaves as an ohmic electrode with respect to hole injection even in the reverse bias. In addition, the presence of the continuous photocurrent indicates that under illumination, free holes are not only generated in the valence band, but also free electrons are generated in the conduction band. This process is possible only when the photon energy of incident light is larger than one-half band gap of ZnO. Accordingly, the onset of the continuous photocurrent should be observed at a wavelength corresponding to half band gap energy. As seen in Fig. 6, the photocurrent is observed at a wavelength shorter than 720 nm, and the photocurrent increases steeply at a wavelength shorter than 360 nm. Thus, the band gap energy of the Co-doped ZnO is estimated to be 3.44 eV. This value is in agreement with literature values of undoped ZnO [13].

Fig. 7 shows the dependence of photocurrent of the three-layer device on a reverse bias voltage. There is a linear relationship between the photocurrent at 400 nm and an applied bias voltage. This is not inconsistent with the theoretical prediction that at a reverse bias voltage the Li-doped NiO is a blocking electrode for the electron injection, but is an ohmic electrode for the hole injection. It should be noted that the photocurrent at 640 nm is proportional to a bias voltage up to 60 V, and then increases exponentially with a bias voltage.

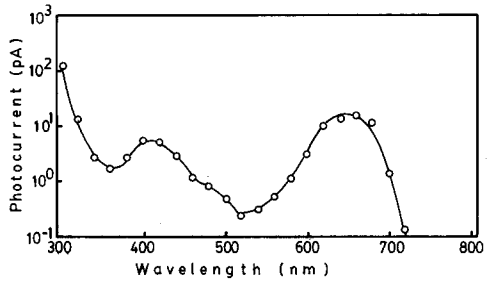

Figure 6 Spectral dependence of photocurrent of the three-layer device kept at a reverse bias voltage of 100 V. The photocurrent is normalized by the photon number of light incident to the device surface.

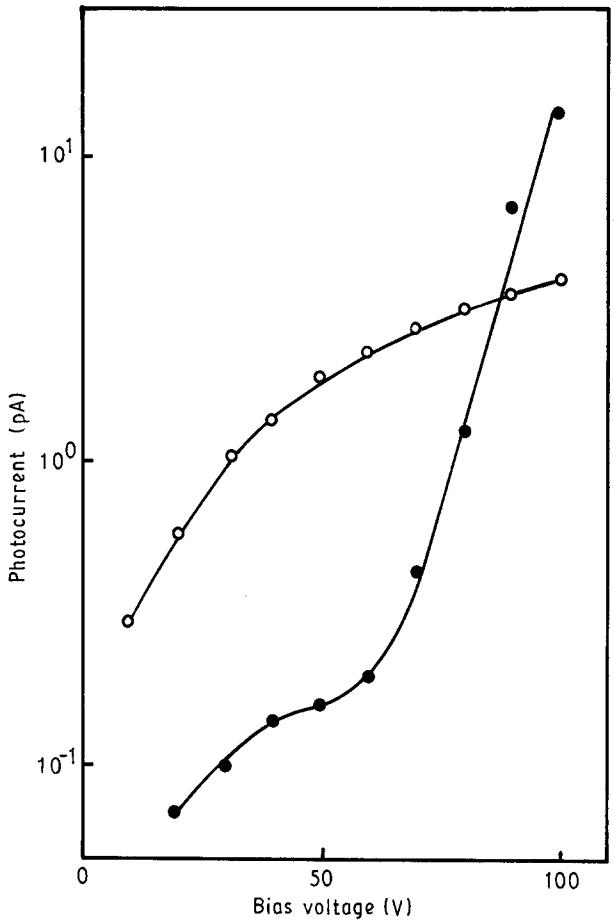

Figure 7 Bias dependences of photocurrents at ○, 400 and ●, 640 nm.

4. Discussion

The photocurrent spectrum around 640 nm is analogous to the broad absorption spectrum around 610 nm, except for the absence of fine structure at 570 and 660 nm. This implies that the generation of free electrons in the conduction band occurs by the transition from the ground states, $^4A_2(F)$, to the excited states, $^4T_1(P)$. Two mechanisms are proposed for the generation of free electrons: (1) the excited states of Co^{2+}, $^4T_1(P)$, are located in the conduction band and then the excited states, $^4T_1(P)$, emit an electron into the conduction band, or (2) the excited states, $^4T_1(P)$, lie below the bottom of the conduction band, and an electron is thermally emitted into the conduction band from the excited states, $^4T_1(P)$. The latter is referred to as photothermal ionization. Recently, photoluminescence from $^4T_1(P)$ to $^4A_2(F)$ was found at 4.2 K by Schulz and Thiede [9]. The presence of photolumine-

scence leads to the conclusion that mechanism (2) is valid.

In addition to the above mechanism, there is a possibility of direct photoionization of the Co ion to the conduction band. In addition, the presence of the continuous photocurrent suggests that holes are generated in the valence band by the charge transfer from the valence band to Co ions. Consequently, we consider the possibility of photoionization by direct transition from Co ions to the conduction band, and the possibility of charge transfer from the valence band to Co ions, on the basis of group theory. The host material of ZnO has the wurtzite structure, space group $P6_3mc = C_{6v}^4$, and the bottom of the conduction band and the top of the valence band exist at the Γ point of the Brillouin zone [14, 15]. For simplicity, we take into account the transitions between Co ions and the conduction (or valence) band at the Γ point. At the Γ point, the irreducible representation of the conduction band minimum is $E_{1/2}$ in the double group $\overline{C_{6v}}$. Similarly, the irreducible representation of the maximum of the valence bands A and B is $E_{1/2}$ and $E_{3/2}$ in the double group $\overline{C_{6v}}$, respectively [9]. In ZnO, Co ions substituted for Zn sites undergo stronger trigonal distortion, so that electronic states of Co ions can be characterized by the irreducible representation in the double group $\overline{C_{3v}}$ including the spin-orbital interaction [7]. For host ZnO, the irreducible representation of $E_{1/2}$ in $\overline{C_{6v}}$ (the bottom of the conduction band and the top of the valence band A) corresponds to $E_{1/2}$ in $\overline{C_{3v}}$, and $E_{3/2}$ in $\overline{C_{6v}}$ (the top of the valence band B) is split into $E_{3/2} + E_{1/2}$ in $\overline{C_{3v}}$. For the electric dipole transition, the electric dipole operator, er, is transformed as A_1 for $\mathbf{E}\|c$, and as E for $\mathbf{E}\perp c$.

For the photoionization, $Co^{2+} \rightarrow Co^{3+} + e^-$ (conduction band) at room temperature, two levels of the ground states, $E_{1/2}$, and the states, $E_{3/2}$, lying at 5.4 cm^{-1} above the ground states, must be considered as the initial states derived from $^4A_2(F)$ in Td symmetry [8]. The following relationship is obtained: $E_{1/2} \times A_1 = E_{1/2}$, $E_{3/2} \times A_1 = E_{3/2}$, $E_{1/2} \times E = E_{1/2} + E_{3/2}$, and $E_{3/2} \times E = 2E_{1/2}$. According to the selection rule, the electric dipole transition from the ground states $E_{1/2}$ to the conduction band are allowed for both the cases of $\mathbf{E}\|c$ and $\mathbf{E}\perp c$, and that from $E_{3/2}$ to the conduction band is allowed only for $\mathbf{E}\perp c$. The above selection rule permits the direct optical transition from Co^{2+} ions to the conduction band.

For the charge transfer processes, $Co^{2+} + e^-$ (valence band) $\rightarrow Co^+$, and $Co^{3+} + e^-$ (valence band) $\rightarrow Co^{2+}$, the initial states correspond to $E_{1/2}$ for the valence band A and $E_{1/2} + E_{3/2}$ for the valence band B. Using the above selection rule, the allowed final states are $E_{1/2}$ and $E_{3/2}$. All levels of Co^{2+} ion are characterized by the irreducible representation of $E_{1/2}$ and $E_{3/2}$. Thus, not only the ground states but also electronically excited states are generated by the charge transfer from the valence band to Co^{3+} ions. In contrast, no electronic states of Co^+ belong to the irreducible representation $E_{1/2}$ and $E_{3/2}$. Therefore, charge transfer from the valence band to Co^{2+} is forbidden.

Besides photothermal ionization, photoionization by the transition from Co^{2+} ions to the conduction band can contribute to the photocurrent. The threshold energy of the photoionization process is larger than that of the photothermal ionization because the electronic excited states of Co^{2+}, $^4T_1(P)$, are located below the bottom of the conduction band. As seen in Fig. 6, therefore, the photocurrent at a wavelength shorter than 500 nm is mainly due to the photoionization process. The peak of the photocurrent at 410 nm seems to be associated with the photoionization process, although the origin of the peak cannot be assigned at the present stage. By taking into account the above theoretical consideration, we propose a mechanism for the occurrence of the continuous photocurrent. Free electrons and Co^{3+} ions are generated by the photothermal and direct ionization processes. Subsequently, free holes in the valence band and Co^{2+} ions are again generated by the charge transfer from the valence band to the generated Co^{3+} ions.

The photocurrent at around 640 nm is explained by the photothermal ionization: electrons are thermally emitted into the conduction band from the electronic excited state of Co^{2+}, $^4T_1(P)$. Under this condition, the barrier height for thermal emission from localized states is reduced by applying an electric field. Such a field effect on the carrier transport may approximately be explained by the Pool–Frenkel model [16] in which current is expressed as $I = I_0 \exp(\mathbf{E}^{1/2}/2kT)$, where $\mathbf{E}$ is the electric field in the insulator bulk. Although it is difficult to obtain an accurate bias dependence of the photocurrent in the small bias range of 60 to 100 V, the bias dependence of the photocurrent at 640 nm is qualitatively consistent with interpretation in terms of thermal emission from localized states.

References

1. G. JACKSON, *Opt. Acta.* **16** (1969) 1.
2. Y. SUEMUNE, *Jpn. J. Appl. Phys.* **22** (1983) 1669.
3. B. W. FAUGHNAN, *Phys. Rev.* **B4** (1971) 3623.
4. Y. M. KSENDZOV and I. A. DRABKIN, *Fiz. Tverd. Tela (Leningrad)* **7** (1965) 1884 [*Sov. Phys.—Solid State* **7** (1965) 1519].
5. J. HUGEL and C. CARABATOS, *J. Phys.* **C16** (1983) 6713.
6. M. SUZUKI, *Phys. Rev.* **B39** (1989) 2312.
7. H. A. WEAKLIEN, *J. Chem. Phys.* **36** (1962) 2117.
8. P. KOIDL, *Phys. Rev.* **B15** (1977) 2493.
9. H. J. SCHULZ and M. THIEDE, *ibid.* **B35** (1987) 18.
10. A. J. BOSMAN and H. J. van DAAL, *Adv. Phys.* **19** (1970) 1.
11. D. ADLER and J. FEINLEIB, *Phys. Rev.* **B2** (1970) 3112.
12. Y. KANAI, *J. Phys. Soc. Jpn* **24** (1968) 956.
13. Y. S. PARK, C. W. LITTON, T. C. COLLINS and D. C. REYNOLDS, *Phys. Rev.* **B143** (1966) 512.
14. H. VENGHAUS, P. E. SIMMONDS, J. LAGOIS, P. J. DEAN and D. BIMBERG, *Solid State Commun.* **24** (1977) 5.
15. D. G. THOMAS, *J. Phys. Chem. Solids* **15** (1960) 86.
16. M. IEDA, G. SAWA and S. KATO, *J. Appl. Phys.* **42** (1971) 3737.

Received 21 October 1991
and accepted 9 January 1992